Hindawi
Geofluids
Volume 2022, Article ID 1775049, 16 pages
https://doi.org/10.1155/2022/1775049

Research Article

The Progressive Failure Mechanism of the Tunnel-Slope System under Rainfall: An Experimental Investigation

Qinglei Jiao[1,2], **Yingchao Wang**[1,3] and **Wen Jiang**[3]

[1]*State Key Laboratory for Geomechanics and Deep Underground Engineering, China University of Mining and Technology, Xuzhou, Jiangsu 221116, China*
[2]*T. Y. Lin International Engineering Consulting (China) Co. Ltd. Xuzhou Branch, Xuzhou, Jiangsu 221116, China*
[3]*School of Mechanics and Civil Engineering, China University of Mining and Technology, Xuzhou, Jiangsu 221116, China*

Correspondence should be addressed to Yingchao Wang; wangyingchao@cumt.edu.cn

Received 8 April 2022; Accepted 11 August 2022; Published 22 September 2022

Academic Editor: Mohammed Fattah

Tunnel excavation has always been an important reason for the stability failure of the tunnel-slope system at the portal section. In case of rainfall, it is likely to cause serious disasters such as tunnel vault collapse, water inrush from the tunnel face, and slope slip. In this study, the Sunjiaya tunnel of the Daping slope group was taken as the engineering background, and the tunnel model experiment system under the condition of rainfall and groundwater seepage was designed independently to explore the failure laws of slope instability induced by tunnel excavation under the condition of rainfall. Meanwhile, a fiber grating monitoring system was also used to measure the displacement, water content, earth pressure, and seepage pressure at different positions of the tunnel-slope system in the process of tunnel excavation under the condition of rainfall. The results show that the slope instability caused by rainfall infiltration is gradual. At the beginning of rainfall, the rainfall infiltration has little effect on the stability of the tunnel-slope system and then gradually increases with the continuous rainfall. Finally, the slope surface is uneven, and the phenomenon of gully and surface flow is serious. The foot of slope moves back continuously, resulting in overall collapse. Moreover, during the process of tunnel excavation, the cracks on the tunnel vault of the unburied tunnel lining develop in quadratic along the tunnel excavation direction, and the closer to the excavation section, the larger the collapse range. Finally, there is an integral collapse of the vault of tunnel excavation section. In addition, variation laws of parameters in the tunnel-slope system also provide an important explanation for the hysteresis of the stability failure of the tunnel-slope system. The results have important guiding significance for the stability of the tunnel-slope system during construction.

1. Introduction

When constructing tunnels in the central and western regions in China, it is inevitable to build tunnels in the slope because of various reasons such as the particularity of engineering, route planning, and incomplete survey quality, etc. There is often a "tunnel-slope" interaction at the entrance and exit of the tunnel when the tunnel is under construction [1]. Tunnel excavation destroys the stress balance and reduces the stability greatly [2]; in case of rainfall, it is easy to induce the creep deformation of the slope and even the overall slide [3–5]. Moreover, after the slope instability, the tunnel will have cracks, deformation, and even vault collapses [6, 7], which will seriously affect the construction safety and the progress of engineering. Therefore, it is of great significance to study the influence of tunnel excavation on slope stability under the condition of rainfall to ensure the engineering safety and construction quality.

In recent years, the theoretical analysis of the interaction between the tunnel and slope has developed rapidly [8], which is the important means to evaluate the stability of the tunnel-slope system. Many useful theories, such as the transmitting coefficient method [9] and the limit analysis method [10], have been applied to reveal the formation mechanism and the failure mode of tunnel structure in slope areas. Moreover, in the analysis of the tunnel-slope interaction, the theory of the

beam on elastic foundation is also often widely used [11]. At present, the finite element method is generally used to solve the problem of elastic foundation beam. However, the finite element method has a large amount of calculation and requires many parameters, which often results in a large difference between the simulation results and the actual values [12, 13]. Therefore, the slip line theory provides a new idea to evaluate the stability of the tunnel-slope system. It plays an important role in the derivation of the disturbance range caused by the tunnel excavation and the minimum safe distance between the tunnel vault and slip zone [14]. Although these theories for evaluating the stability of the tunnel-slope system are mature and perfect, they still have many disadvantages. For example, the calculation process is complex and difficult to solve, the actual engineering parameters are imperfect, and the failure process of the slope instability cannot be observed.

The geomechanical model is also one of the important measures to predict the instability of the tunnel-slope system. Relevant experts and scholars in Japan first summed up the geological model of the tunnel deformation in the slope areas. After that, Ma [15] put forward five kinds of geological structure models of the slope disease and the tunnel deformation by investigating the deformation of the main railway tunnels in the mountain areas of China. On this basis, Tao [16] theoretically analyzed the stress mode and the deformation mechanism of tunnel under the combined action of slope thrust and ground pressure. Wu [17] further enriched the geomechanical model of the tunnel-slope system and finally obtained the interaction law of the tunnel-slope system. According to the above, when dividing the geological structure model of slope diseases and tunnel deformation, most experts mainly consider the rock structure characteristics, the spatial position relationship between the tunnel and the slope, and the time effect of surrounding rock deformation [18–20]; the combined influence of engineering disturbances and hydrogeological conditions are rarely considered.

Because the large-scale model experiment can be closely combined with the actual engineering background, many experts and scholars often use this method to study the stability of tunnels in landslide areas and have made a series of results. S. Ganger [21] first discussed the slope sliding problems caused by tunnel excavation construction through model experiments and summarized the causes of diseases. Then, Tao [22] and Wu et al. [23–25] studied the interaction mechanism between slope deformation and tunnel stress in a landslide section, the variation laws of tunnel lining pressure, and the deformation characteristics of the tunnel and slope through different model experiments. On the basis of previous studies, Zhang et al. [26], Yin et al. [27], and Chen [28] obtained the stress characteristics and disaster prevention measures of tunnel damage caused by landslide instability during the operation period by studying the reinforcement effect of anchor cable of different numbers of tunnels, the stress and deformation characteristics of self-anchored reinforcement structure, and the arrangement of rear embedded antislide piles at different spacing, which provided a reference for the tunnel design in the landslide areas. At present, more and more scholars have added more field conditions to the model experiment. By studying the landslide instability induced by rainfall infiltration, Ai et al. [29] and Gao et al. [30] have obtained the catastrophic evolution processes of the tunnel-slope system and the stress characteristics of the tunnel. Through the shaking table model experiment of the tunnel structure, Li et al. [31] obtained the acceleration characteristics, formation deformation laws, and internal force distribution of the shallow buried bias and non-bias tunnel.

Other methods, such as the numerical simulation analysis and the engineering monitoring, are often used to analyze this problem [32, 33]. Xing et al. [34] investigated the influence of the tunnel excavation on the stability of the surrounding rock mass through a three-dimensional (3D) numerical analysis under the combined action of complex geologies and engineering disturbances. The displacement and strength degradation areas around the excavation areas were discussed in detail. This study provides effective suggestions for the stability evaluation and reasonable support after the tunnel excavation in complex geology. Through numerical simulation and model experiment, Zhang et al. [35] found that the influence range of the slope deformation caused by tunnel excavation is 1.5 times that of the tunnel span. Gattinoni et al. [36] reconstructed the conceptual model of both the slope dynamics and the tunnel construction at first. Then, based on numerical simulation, it is concluded that long and heavy rainfall can contribute to slope instability much more than tunnel excavation itself. Qin [37] studied the stability of slope before and after the tunnel excavation through the actual tunnel engineering monitoring, analyzed the failure mechanism of the side slope during tunnel construction, and finally concluded that the excavation of the portal section had the greatest impact on the stability of the slope.

To sum up, previous studies on this problem mainly use theoretical analysis and numerical simulation [38] and rarely consider the impact of rainfall during the tunnel excavation. Moreover, because the model experiment often requires specific instruments and equipment, the model experiment has certain difficulty, and it is difficult to obtain the experimental law, the results of the model experiment are relatively backward compared with those of other research methods. Therefore, this study intends to use the independently designed multifunctional platform for tunnel model experiment under the action of rainfall and groundwater seepage to carry out the model experiment research. Moreover, the fiber Bragg grating (FBG) monitoring system is used to measure the water content in different positions and depths of the tunnel-slope system, as well as the change laws of displacement, soil pressure, and seepage pressure in the upper part of the tunnel vault during the whole rainfall process. This study could provide an important basis for tunnel safety in construction in the slope area.

2. The Designment of the Model Experiment

2.1. Determine Similar Parameters. In this model experiment, the Sunjiaya tunnel of the Daping slope group was taken as the engineering background. Typical slope sections were selected for the model experiment [39, 40]. According to the actual engineering size and the model experiment box specifications, the geometric similarity ratio and the bulk similarity constant were selected in this experiment.

Table 1: The proportion of similar soil materials.

Name	Material	Ratio
Bedrock	Clay, lime	7 : 3
Slope	Medium sand, clay, talcum powder, water	11 : 3 : 4 : 2
Sliding zone	Laying talcum powder and water with double-layer plastic film	2 : 1
Tunnel lining	PVC pipe	With a dimeter of 15 cm

$$S_L = 80, \quad S_\gamma = 1. \tag{1}$$

Based on the analysis of the seepage theory and the runoff theory, the Weber criterion can be used as the rainfall similarity criterion for the rainfall infiltration experiment. The relationship between the rain intensity scale and the geometric scale can be deduced as follows [41].

$$S_u = S_l^{-1/2}. \tag{2}$$

In the model experiment, the S_l is 80, and the similar scale of rain intensity S_u is 0.11. The rain type used in this model experiment is moderate rain (30 mm/d).

2.2. Choose Similar Materials. Based on mechanical parameters of prototype soil of the Sunjiaya tunnel of the Daping slope group and previous experiments [28, 29], the similar soil materials are proportioned in Table 1.

2.3. The Model Experiment Device. The independently designed tunnel model experiment system under the action of rainfall and groundwater seepage is composed of a model experiment box, artificial rainfall simulation system, groundwater seepage simulation system, tunnel excavation simulation system, ground stress loading system, and intelligent data collection system. It belongs to a multifunctional experiment platform.

The model box [42] is shown in Figure 1; the internal net size of the model experiment box is 2.5 m × 1.0 m × 1.4 m (length × width × height). There are two tunnel openings of different sizes on the front and side of the model box. The diameter of the front tunnel excavation hole is 30 cm, and the diameter of the side tunnel excavation hole is 20 cm. In the model experiment, the box can be adjusted using the lifting angle reasonably within the range of 0~30° according to the experiment requirements (the angle control accuracy is ± 1°, and the maximum lifting mass is 20 t). In addition, visual glasses are installed on the side of the model box, which is convenient to observe the phenomenon changes in the model experiment in real time. Four pieces of visualization glasses are installed on the side of each model box, and the size of each piece of visualization glass is 80 cm × 40 cm (length × width).

The artificial rainfall simulation system [42] is mainly composed of the rainfall device and the rainfall control system, as shown in Figures 2 and 3. In the rainfall control system, the appropriate rainfall intensity can be selected in the rain intensity selection areas according to the experiment requirements. There are four rainfall modes set in this system: light rain (5~10 mm/d), moderate rain (10~25 mm/d), heavy rain (25~50 mm/d), and torrential rain (50~70 mm/d). The rainfall

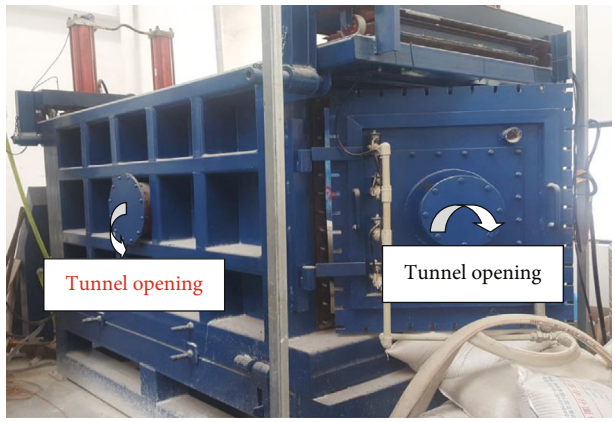

Figure 1: The model box [42].

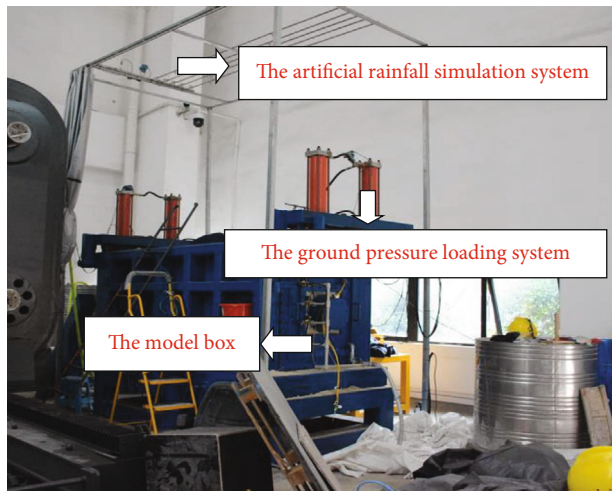

Figure 2: Three-dimensional tunnel model experiment system under rainfall and groundwater seepage [42].

and the dynamic rainfall curve can be viewed in the statistical rainfall curve column and the report viewing column in real time.

The rainfall device mainly adopts nozzle type sprayers, with a total of 15 sprayers, which are arranged in three columns with a spacing of 15 cm. Under the regulation of the rainfall control system, the rainfall sprinkler can automatically adjust the effective rainfall height within the range of 0~2 m and the spraying range (0~3 m^2).

The groundwater seepage simulation system [42] is mainly composed of the intelligent pressurized water supply and the drainage system, as shown in Figure 4. In the intelligent

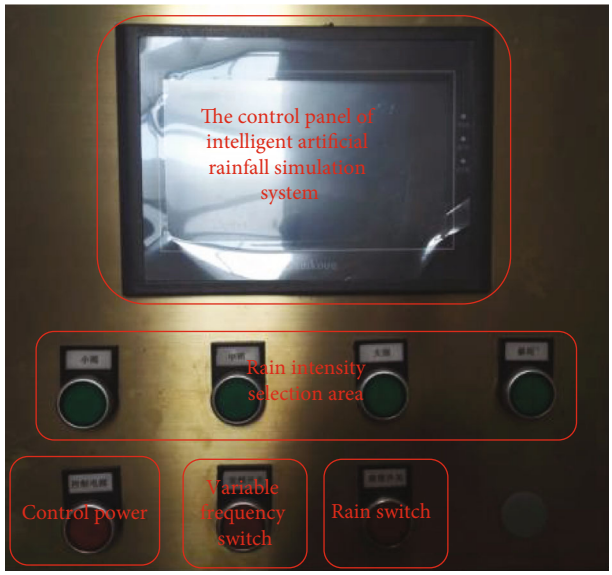

Figure 3: The rainfall control system.

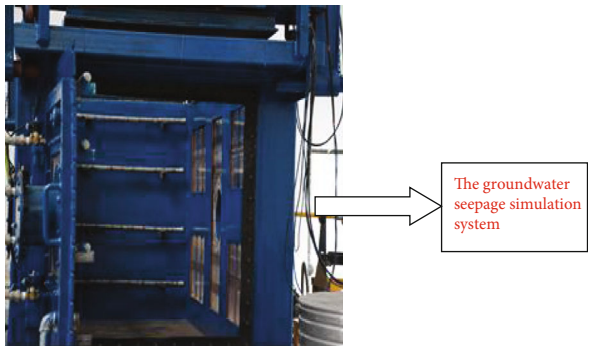

Figure 4: The groundwater seepage simulation system [42].

Figure 5: The tunnel excavation simulation system [42].

Figure 6: The ground stress loading system [42].

pressurized water supply system, the water supply conditions required by different experiments are mainly simulated by the layered water supply device. Among them, the layered water supply device is mainly arranged in four layers inside the model box. The total length of each layer of the water supply pipe is 80 cm, the diameter is 20 mm, and 2 mm small holes are distributed every 5 cm on the water pipe, which can meet the experiment water level requirements of 0.2 m minimum water level and 1.3 m maximum water level.

Through the combination of the intelligent data collection system and the groundwater seepage simulation system, parameters such as the pressure value of water supply pipeline of 0~0.6 MPa, the water supply flow of 0~08 m^3/h, and the soil water content from 0 to 100% can be automatically collected. After the experiment is ended, the drain solenoid valve and multiple drain valves or the total drain port are opened according to the water level, and the water will be automatically discharged into the waste water collection box. The drainage system can stop working automatically when the drainage pipe does not emit water.

The tunnel excavation simulation system [42] is shown in Figure 5. The tunnel excavation device has four specifications of the excavation radius, including 15 cm, 20 cm, 25 cm, and 30 cm. The height of the support can be adjusted upward and downward, and the adjustment range is 0~130 cm. The excavation method adopts automatic drilling with an electric drilling rig, which can ensure the characteristics of the stability and the accuracy of excavation footage in the process of tunnel excavation.

The ground stress loading system [42] is mainly composed of two compression plates, each of which has an area of 0.3 m^2, as shown in Figure 6. The maximum pressure control range is 50 mm, and the maximum simulated ground stress is 1 MPa. It can remain stable for 7 days after the end of the pressurization.

The intelligent data collection system is mainly composed of the intelligent data collection system and the intelligent data analysis system, as shown in Figure 7. In the intelligent data collection system, the data collection is mainly carried out by the FBG demodulator and FBG monitoring elements, as shown in Figure 8. Among them, the FBG demodulator is a

Figure 7: The intelligent data collection system [43].

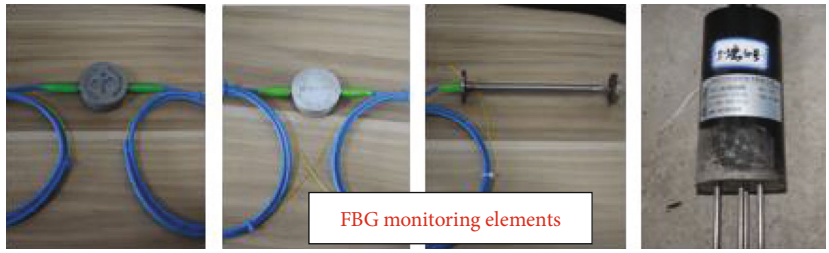

Figure 8: FBG monitoring elements [43].

universal 16-channel wavelength demodulator, which has the functions of 1525~1565 nm wavelength measurement range, 100 Hz wavelength demodulation rate, and the maximum capacity of 80 FBG sensors in a single channel. The main monitoring elements are fiber grating displacement gauge (accuracy: ±0.05 mm, range: 0~40 mm), fiber grating earth pressure gauge (range: 0~1.6 MPa), and fiber grating seepage pressure gauge (range: 0~1.2 MPa). The water monitoring adopts a TDR III-type soil moisture sensor (accuracy (0~50%RH): ± 2%, range: 0~100%) in the slope. Through the intelligent data collection system and the intelligent data analysis system, the real-time monitoring and the dynamic analysis of monitoring data can be realized.

2.4. Experiment Steps

2.4.1. Making Bedrock. The bedrock is simulated with the mixture of clay and lime, and the bottom surface is made into a plane. Moreover, the model box is paved in layers every 10 cm and compacted layer by layer.

2.4.2. Paving Strip. As shown in Figure 9, the sliding material is simulated by the mixture of talcum powder and water in the middle of the double-layer plastic film. The composition ratio is 2 : 1, and the thickness of the strip is 5 cm.

2.4.3. Burying Lining. As shown in Figure 10, the supporting structure of the tunnel portal section is simulated by a PVC pipe. According to the geometric similarity ratio, the PVC pipe with a diameter of 20 cm, a length of 20 cm, and a thickness of 0.3 cm is selected for simulation.

2.4.4. Making Slope. The slope is simulated by the mixture of medium sand, clay, talc powder, and water. After mixing the simulated materials evenly, each 10 cm layer was paved into the model box and compacted layer by layer.

Figure 9: The paving of sliding belt materials.

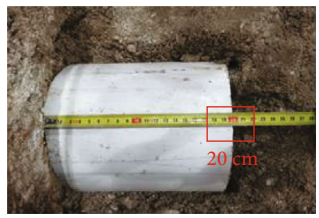

Figure 10: The embedment of the PVC pipe.

2.5. The Embedding of Sensors. Fiber grating sensors are mainly arranged in the model box in two layers, in which

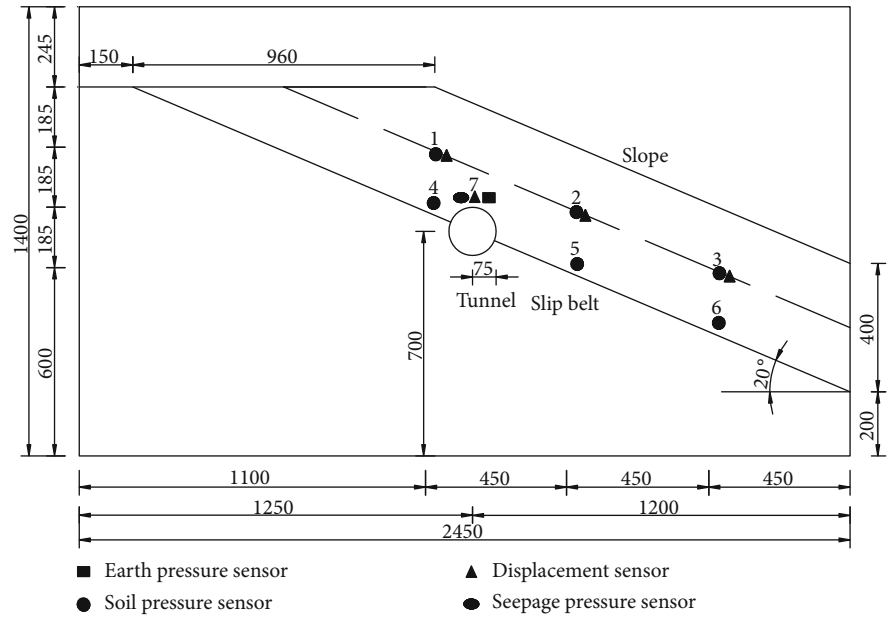

Figure 11: The section view of the tunnel-slope system model experiment (unit: mm).

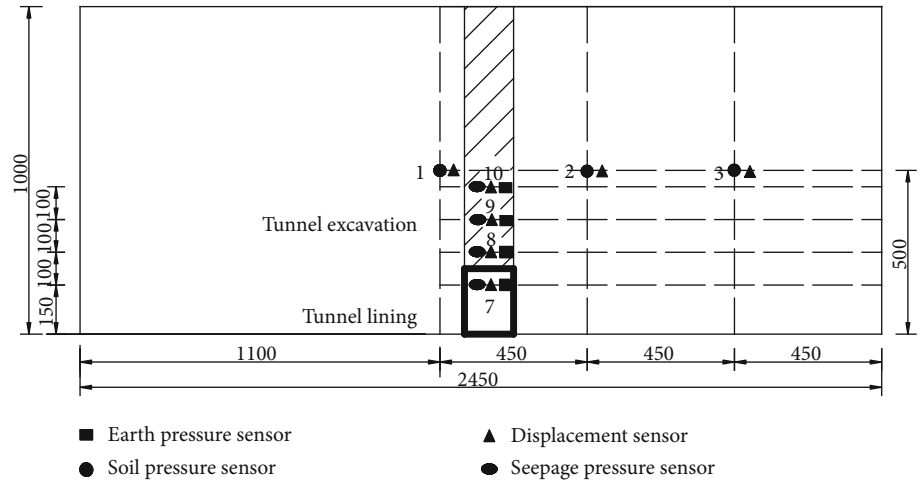

Figure 12: The top view of the tunnel-slope system model experiment (unit: mm).

those sensors are arranged parallel to the slide and 5 cm above the slide in the first layer. They are mainly arranged at the front, middle, and back edges of the slope. The second layer is arranged in the middle of the slope and is parallel to the first layer.

In the direction of the tunnel excavation, three sensors (displacement sensor, seepage pressure sensor, and soil pressure sensor) are arranged at 1R on the top of the tunnel vault along the direction of the tunnel axis. Specific arrangement can be seen in Figures 11 and 12.

3. The Analysis of Stability Changes of the Tunnel-Slope System during Rainfall

3.1. The Analysis of Stability Changes during Tunnel Excavation. Under rainfall conditions, tunnel excavation is mainly divided into the following three stages: (1) the development stage of rainfall infiltration, (2) the development stage of the seepage channels inside the tunnel, and (3) the development stage of the tunnel arch collapse. To facilitate the control of excavation footage, the current footage of each excavation is 3 cm, which is equivalent to 3 m of the blasting excavation in actual construction. In this experiment, the electric drill is used to excavate in the form of full section for 9 times in total. When the tunnel is excavated to the ninth time, the whole tunnel vault collapses suddenly and the experiment ends.

3.1.1. The First Stage: The Development Stage of Rainfall Infiltration. During the first and second tunnel excavation (as shown in Figures 13(a) and 13(b)), due to the short rainfall time, the rainwater only infiltrates to the shallower position of the slope. At this time, the tunnel wall and the tunnel face are dry and smooth without falling blocks and sand. The overall self-stability of the tunnel is good.

(a) First excavation

(b) Second excavation

(c) Third excavation

(d) Fourth excavation

Figure 13: Continued.

(e) Fifth excavation

(f) Sixth excavation

(g) Seventh excavation

(h) Eighth excavation

Figure 13: Continued.

(i) Ninth excavation

(j) Water inrush from tunnel

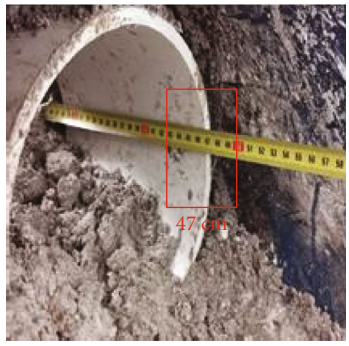

(k) Tunnel excavation footage

Figure 13: The analysis of stability of the tunnel during excavation.

3.1.2. The Second Stage: The Development Stage of the Seepage Channel inside the Tunnel. The tunnel face after the third excavation is shown in Figure 13(c); after 30 minutes of rainfall, the tunnel wall and the tunnel face are in a wet state. Under the action of the excavation disturbance, the tunnel face transits from a smooth to rough state continuously. At this time, a small amount of water seeps out from the tunnel face at times, which shows that the seepage channel in the tunnel-slope system is gradually formed during the tunnel excavation process, but the development is limited. Blocks and sand have fallen off from the vault and the arch shoulder of the tunnel, and the stability of the tunnel excavation section is gradually decreased, but the stability of tunnel lining structure support is still good. The face after the fourth excavation is shown in Figure 13(d). After 45 minutes of rainfall, the seepage channel inside the tunnel-slope system has further developed. The amount of water infiltration on the tunnel face is increasing, and the water quality is turbid. At this time, the phenomenon of falling blocks and sand is serious. The face after the fifth excavation is shown in Figure 13(e). After 1 h of rainfall, the tunnel wall and the tunnel face are wetter than before, and the tunnel face is uneven. At this time, the phenomenon of falling blocks and sand in the tunnel is becoming more and more serious, and the self-stability of the tunnel excavation section is decreasing continuously, but the tunnel lining structure support is good. The face after the sixth excavation is shown in Figure 13(f); the mud water mixture at the front section of the tunnel face continues to flow out, which seriously blocks the tunnel excavation and requires to be cleaned manually. This shows that the internal seepage channel of the tunnel-slope system has been formed and is still developing rapidly. At this time, the stability of the tunnel excavation section is bad, but the stability of the support of tunnel lining structure is still relatively stable.

3.1.3. The Third Stage: The Development Stage of Tunnel Arch Collapse. The face after the seventh excavation is shown in Figure 13(g). Under the continuous tunnel excavation and rainfall infiltration, some small-scale collapses occur in the tunnel at times. The self-stability of the tunnel excavation section is worse, but the stability of the support of tunnel lining structure is good. There are no falling blocks, sand, or collapses in the portal section, which is obviously different from that in the unsupported part. The tunnel face after the eighth

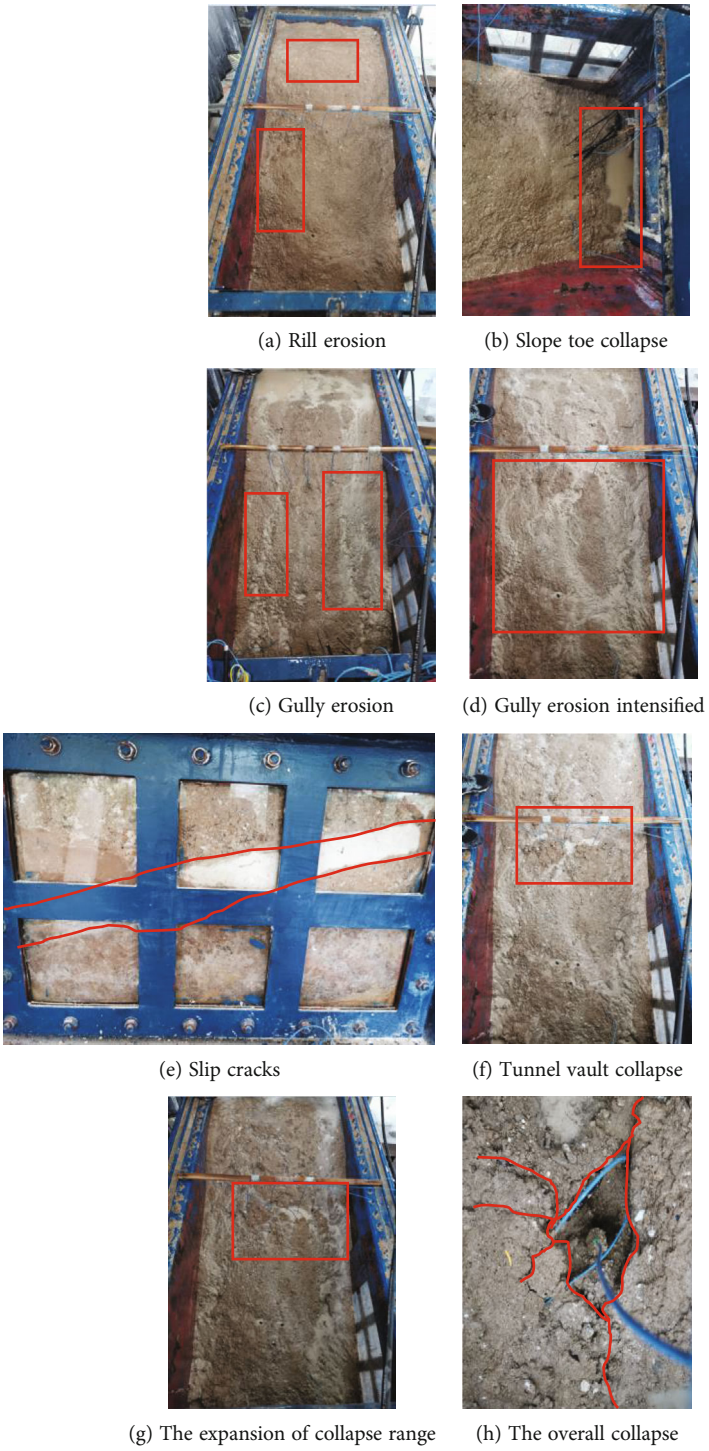

(a) Rill erosion (b) Slope toe collapse

(c) Gully erosion (d) Gully erosion intensified

(e) Slip cracks (f) Tunnel vault collapse

(g) The expansion of collapse range (h) The overall collapse

Figure 14: The analysis of the slope instability during rainfall.

excavation is shown in Figure 13(h); during the tunnel excavation, the collapse ranges of the tunnel face and tunnel vault are expanding constantly. The mud water mixture in the tunnel face gushes out continuously, the water quality is turbid, and the flow velocity is fast. The face of the ninth excavation is shown in Figure 13(i). During the excavation of the tunnel, the collapse ranges of the tunnel face and vault continue to expand. After about 5 min, an integral collapse occurred on the tunnel vault, with the shape of a quadratic parabola. The rainwater mixed with collapses gushes out from the tunnel face constantly, and the water quality is turbid, as shown in Figure 13(j). After a few minutes, the water is clear. The total excavation footage is 47 cm, as shown in Figure 13(k). So far, the experiment is over.

3.2. The Analysis of the Slope Instability Process. In the early stage of rainfall, the water content of the slope is less. With the continuous infiltration of rainwater, the water content of

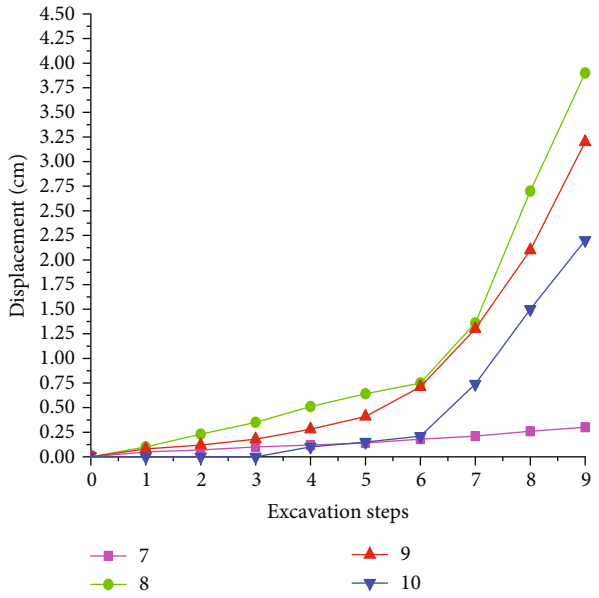

Figure 15: The changes of the displacement of the tunnel vault with excavation steps.

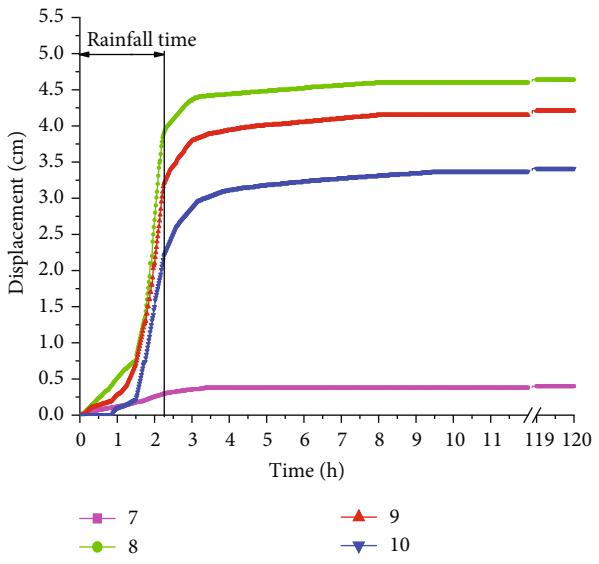

Figure 16: The changes of the displacement of the tunnel vault with time.

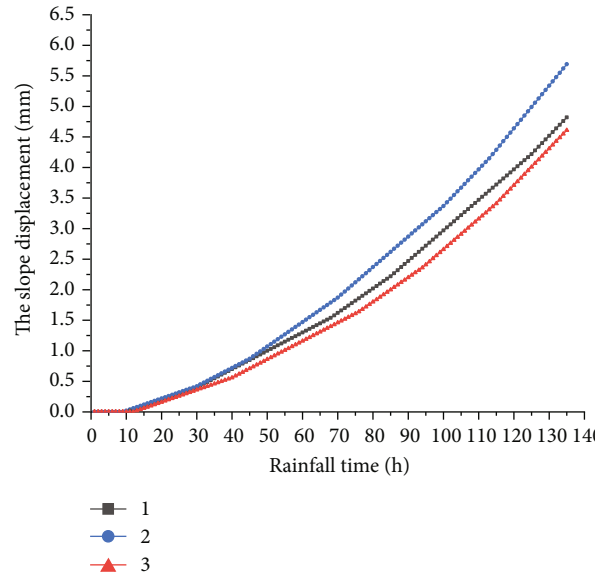

Figure 17: The changes of the slope displacement with rainfall time.

the slope increases continuously. However, due to the large amount of rainwater infiltration in the slope at the beginning, there is almost no obvious response. Besides, the tunnel excavation footage is short, and the excavation disturbance range is small. Therefore, the slope still maintains good stability.

After 30 minutes of rainfall (as shown in Figures 14(a) and 14(b)), the water content of the slope is still increasing. At this time, rill erosion occurs in the slope surface under the constant scouring effect of rainwater. There is also a small amount of water in front of the slope. In addition, there are a few discontinuous cracks on the tunnel vault, and the cracks are developing towards the direction of tunnel excavation. After 40 minutes of rainfall (as shown in Figure 14(c)), the infiltration of the slope gradually starts to decrease, and the water content of the slope tends to be stable. At this time, the slope surface forms gully erosion with a certain depth and width under the scouring effect of rainwater. There is also a small range of collapse at the foot of slope. After 60 minutes of rainfall (as shown in Figure 14(d)), the amount of water accumulated in the gullies is increasing, and the gullies gradually deepen under the continuous scouring effect of rainwater. After 75 minutes of rainfall (as shown in Figure 14(e)), the confluence of the surface flow is also obvious, and there are also a lot of slip cracks near the slip zone. At this time, the damage degree of the slope is developing rapidly.

After 105 minutes of rainfall (as shown in Figure 14(f)), partial settlement occurs in the tunnel vault, resulting in the formation of a puddle in the tunnel vault. Under the continuous excavation, the area of the water puddle is becoming larger and larger, and the amount of water accumulation is also increasing. After 115 minutes of rainfall (as shown in Figure 14(f)), a large amount of water and surface flow can be seen everywhere on the surface of the slope. There are more and more cracks near the slip zone. At this time, the surface of the slope is scoured and eroded seriously. In the later stage of rainfall (as shown in Figure 14(g)), the stability of the tunnel vault is extremely worse, and the collapse section is in the shape of a quadratic parabola and develops continuously to the postexcavation section. Finally, under the action of rainfall infiltration and excavation disturbance, the tunnel vault collapses as a whole, and collapses gush out from the tunnel face continuously; so far, the experiment ends. The collapse range is 13 cm in length and 18 cm in width. Five days after the end of the rainfall, the collapse range is 17 cm in length and 22 cm in width.

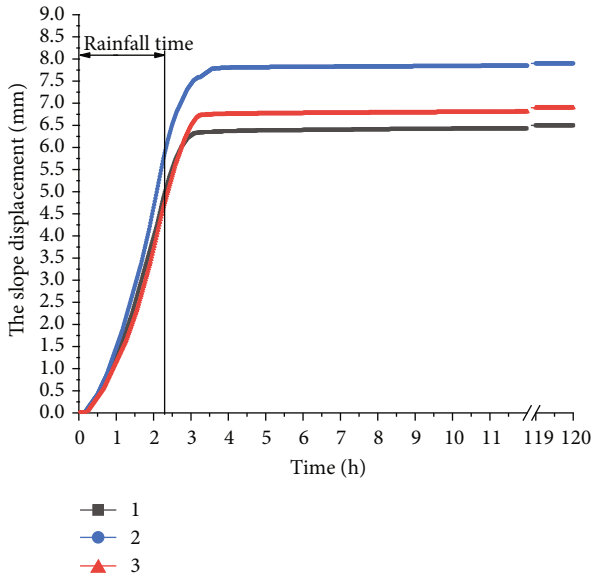

Figure 18: The changes of the slope displacement with time.

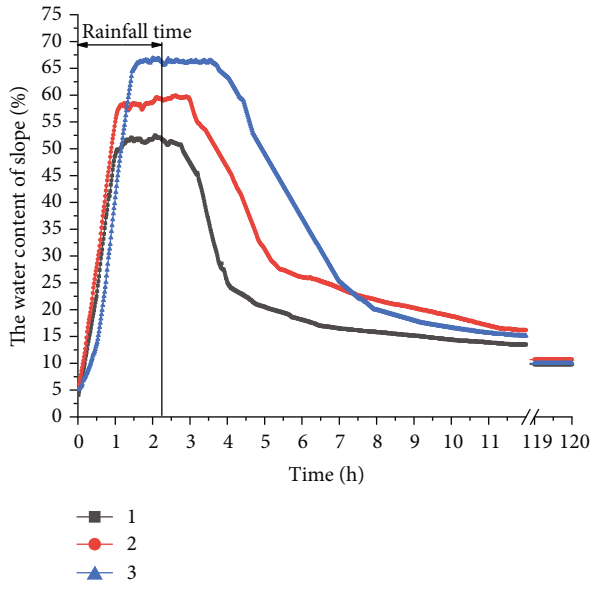

Figure 19: The changes of the upper slope water content with time.

4. The Analysis of Internal Change Laws in the Tunnel-Slope System during Rainfall

4.1. The Analysis of Displacement Changes of the Tunnel Vault. As can be seen from Figure 15, at the early stage of rainfall, rainfall infiltration has little impact on the tunnel stability, and the tunnel has good self-stability. Under the disturbance of tunnel excavation, the displacement of the tunnel vault has a slight change. With the continuous action of rainfall infiltration and tunnel excavation, the displacement of the tunnel vault is on the rise. When the tunnel is excavated to the sixth time, the phenomenon of falling blocks and sand on the vault of tunnel is becoming more and more serious, and the increasing rate of the tunnel vault displacement is accelerating. When

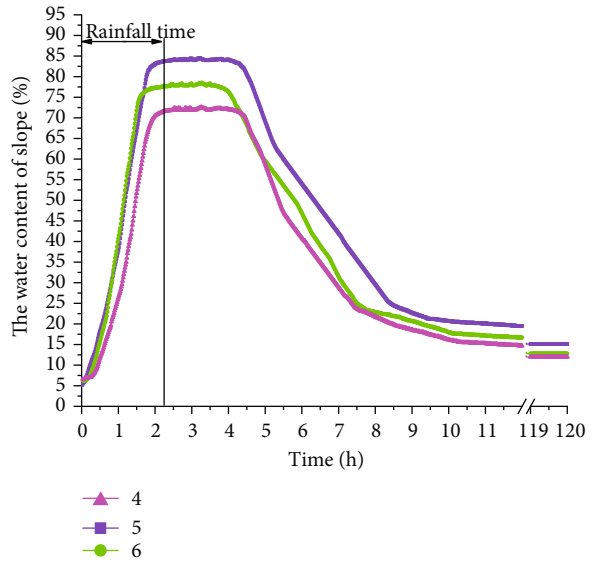

Figure 20: The changes of the lower slope water content with time.

the tunnel is excavated to the seventh time, the tunnel vault collapses in a small range, and the displacement of the tunnel vault shows a rapid upward trend. In the later excavation process, the scope of the tunnel vault collapse is expanding, and the closer it is to the collapse surface, the more obvious the displacement growth trend. However, due to the existence of support structure at the tunnel entrance, the growth trend of displacement is slower than that of the excavation section.

As can be seen from Figure 16, after the end of rainfall, the displacement of the tunnel vault does not stop immediately but still maintains a rapid growth rate. It shows that the collapse and settlement of the tunnel vault induced by rainfall infiltration have the characteristics of hysteresis. A transient pressure arch is formed around the tunnel wall after the end of the rainfall for about two hours. At this time, the stresses of all sides form an equilibrium state, and the settlement of the tunnel vault also gradually becomes stable. Therefore, in the actual construction process of the tunnel, the tunnel lining should be done as soon as possible to make the surrounding rock and the support structure form a whole, to improve the safety of the tunnel excavation section. In addition, the corresponding drainage measures should be set up at the top of the tunnel vault to prevent leakage on the lining surface of the tunnel, which will reduce the structural strength of tunnel lining for a long time.

4.2. The Analysis of Slope Displacement Results. It can be seen from Figure 17 that in the early period of the rain, there is basically no obvious change in the slope displacement, but as the rainfall infiltration continues, the whole slope displacement shows a rising trend. In the process of the experiment, the front door of the slope is closed tightly, which limits the development of the front displacement of the slope to a certain extent. However, the displacement of the middle part of the slope changes the most due to the excavation disturbance. The growth trend of the displacement at the back and front of the slope is relatively slow, but the general rule is similar.

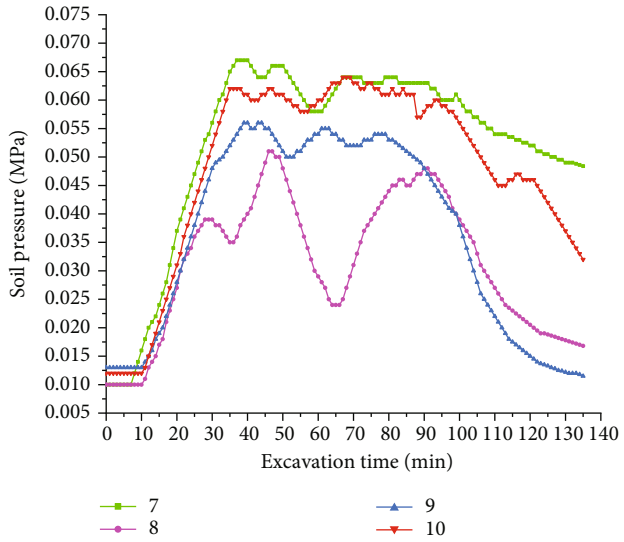

Figure 21: The changes of the soil pressure on the tunnel vault with rainfall time.

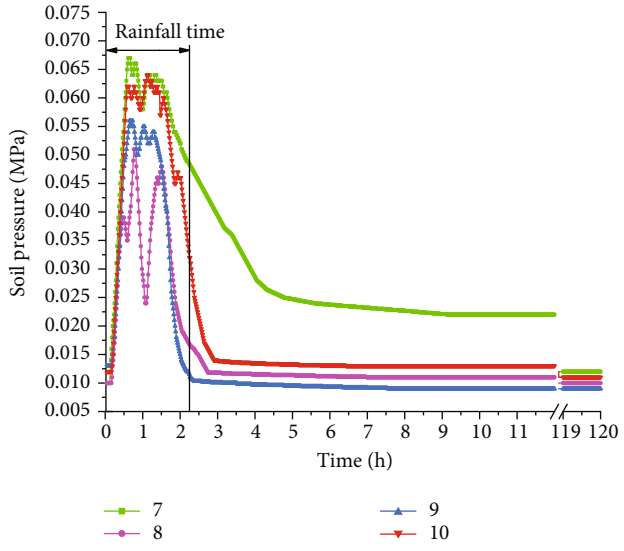

Figure 22: The changes of the soil pressure on the tunnel vault with time.

As can be seen from Figure 18, after the rainfall, the displacement of the slope does not stop developing but continues to keep rising. The result shows that the slope failure induced by the rainfall infiltration has the characteristics of hysteresis. The main reason is that under the effect of the long-term rainfall infiltration, the internal structure of the slope is loose, which makes the strength of the slope become more uneven; the integrity and stability of the slope further decrease, so that the displacement in slope increases in different degrees. After the rain stops for about 2 hours, the displacement in the slope gradually stabilizes.

Therefore, when the tunnel is excavated in the slope area, the slope must be reinforced in advance to prevent the creep deformation and even the overall collapse accident caused by tunnel excavation.

4.3. The Analysis of Water Content Changes in the Tunnel-Slope System. It can be seen from Figures 19 and 20 that the change trend of the water content at different depths of each soil layer in the slope is different in rainfall and after rainfall. In the early period of the rain, due to the fact that the rain seepage needs some time to accomplish, the water content of the upper layer of slope changes obviously and the response speed is fast. However, the water content in the lower layer of slope gradually increases after a period of rainfall infiltration, and the response speed is slow. After about 1 h of the rainfall, the water content at different depths of the slope reaches the peak value and tends to be stable gradually. The main reason is that the infiltration amount is larger than the runoff amount of the slope at the initial period of rainfall. With the continuous rainfall infiltration, when the infiltration amount and runoff amount of the slope gradually become stable, the water content of each layer in the slope does not continue to increase. After the rainfall, the water content in different depths of the slope will not immediately decrease but gradually decrease after a certain period of time, which has a certain degree of "hysteresis characteristics." At the end of the rainfall for 1 h, the water content in the upper layer of the slope decreases rapidly because of the fast speed of rainwater loss. However, due to the slow rate of rainwater loss in the lower slope, the water content in the lower slope can remain relatively stable within 3 hours after the end of rainfall. With the continuous loss of rainwater, the runoff amount of rainwater is larger than the infiltration in the slope, resulting in a rapid downward trend of water content in the lower slope. After 8 hours of the rainfall, the water content of each soil layer finally tends to be the same.

In conclusion, the closer the rainwater infiltration to the slope surface, the faster the response speed and the more obvious the change range, but the shorter the retention time of the peak water content and the peak water content. Correspondingly, the further the rainwater infiltrate is to the slope, the slower the response speed and the longer the retention time of the peak water content. After the end of rainfall, the water content of each layer in the slope will not decrease immediately but gradually decrease after a period of rainfall, which is also one of the important reasons for the instability of the slope after the rain.

4.4. The Analysis of Soil Pressure Changes in the Tunnel-Slope System. As can be seen from Figure 21, in the early period of the rainfall, due to the fact that the impact of tunnel excavation is little, the soil pressure in various parts of the tunnel vault increases continuously under the action of rainwater infiltration. When the water content of the tunnel-slope system tends to be stable, the soil pressure in various parts of the tunnel vault also tends to be stable gradually. When the rainfall is about 50 minutes, the phenomenon of falling blocks and sand on the tunnel vault is serious, resulting in a significant decline of No. 8 earth pressure sensor near the collapse surface. Then, under the continuous infiltration of rainwater, the soil pressure of the tunnel vault shows a rising trend. When the rainfall is about 90 minutes, the stability of the tunnel-slope system is decreasing, the phenomenon of falling blocks and sand in the tunnel is becoming more and more serious, and even small-

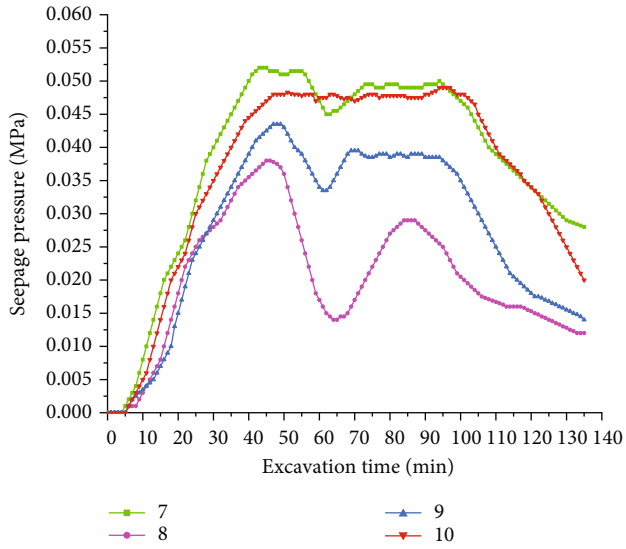

Figure 23: The changes of the seepage pressure on the tunnel vault with rainfall time.

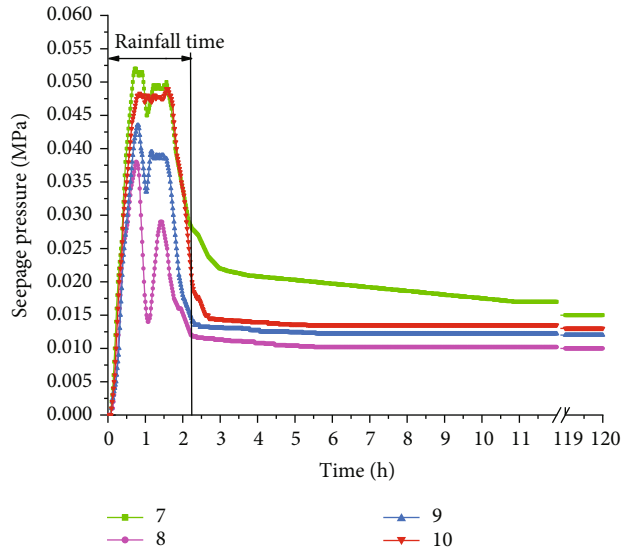

Figure 24: The changes of the seepage pressure on the tunnel vault with time.

scale collapses occur in some sections. At this time, the scope and the degree of collapse areas are expanding, resulting in the decreasing trend of the soil pressure in all sections of the tunnel vault. Finally, the overall collapse of the tunnel vault occurs, resulting in a cliff-like downward trend of soil pressure sensors.

As can be seen from Figure 22, after the rainfall stops, the soil pressure above the tunnel vault does not stop decreasing but continues to decrease with the expansion of the collapse scope and degree of the tunnel vault. After the rainfall stops for about 3 hours, the soil pressure around the tunnel vault gradually comes to stability. It shows that there is a hysteresis in the collapse of the tunnel vault induced by excavation under rainfall conditions, and it is very likely that it will occur after rain when the collapse degree is the largest. However, the stability of the embedded lining is relatively good in the whole rainfall process, and there is no falling sand and collapse phenomenon, which plays an important role in supporting the excavation of the tunnel.

4.5. The Analysis of Seepage Pressure Changes in the Tunnel-Slope System. It can be seen from Figure 23 that the change trend of the seepage pressure and the soil pressure of the tunnel-slope system is similar in the whole rainfall process. In the early period of rainfall, due to the small disturbance of the tunnel excavation, the seepage pressure at all parts of the tunnel vault is rising and gradually tends to be stable under the continuous rainfall infiltration. When the rainfall is about 50 minutes, the phenomenon of falling blocks and sand in the excavation section of the tunnel vault occurs continuously, and even a small section of collapse has occurred, resulting in a temporary downward trend in the seepage pressure of the tunnel vault. After that, under the timely supply of rainwater, it shows a rising trend. When the rainfall is continuing for about 90 minutes, under the joint action of the rainfall infiltration and the tunnel excavation, the phenomenon of falling blocks, sand, and collapses of the tunnel vault is becoming more and more serious. At this time, the seepage pressure of the tunnel vault decreases continuously. During the later excavation of the tunnel, the collapse range extends from the tunnel excavation to the tunnel entrance section. The rainwater flows out from the entrance section constantly with collapses, resulting in a straight-line downward trend of seepage pressure sensors.

As can be seen from Figure 24, after the rainfall stops, the seepage pressure of the tunnel vault does not keep stable but continues to decrease obviously. The cause of this phenomenon is probably that after the rainfall stops, the collapse range of the tunnel vault continues to expand, and a large amount of rainwater flows out from the collapse surfaces and the cracks. After the rainfall stops for about 5 hours, seepage pressure sensors tend to be stable. It shows that the collapse and settlement of the tunnel vault induced by rainfall infiltration have hysteresis. The change laws are basically the same as that of the soil pressure sensors.

5. Conclusions

Through the large-scale physical model experiment, the influence of the excavation disturbance on the stability of the tunnel-slope under rainfall conditions is studied. The main conclusions are as follows:

(1) The collapse process of the tunnel vault caused by tunnel excavation can be described as follows: tunnel excavation → gradual decline in self-stabilizing ability → falling blocks and sand → the internal seepage channel gradually develops → small scale collapse with the water seepage from the tunnel face → the amount of mud water mixture from tunnel face is increasing → the expansion of the collapse scope → the stability of the excavation section is very poor → the integral collapse of the excavation section in the form of a quadratic parabola → water inrush

from the tunnel face. And in the excavation process, the collapse degree of the first excavation section will expand with the continuous excavation of the second section; in other words, the influence and development of each excavation section are closely related. However, in the whole process of rainfall, the stability of the embedded part of tunnel portal lining is relatively good, and there are no collapse and falling sand. Therefore, in the construction process of the tunnel portal section in the slope area, tunnel lining support is particularly important.

(2) The process of the slope instability caused by the rainwater infiltration can be described as follows: rainfall infiltration → rill erosion → slope toe collapse → gully erosion → gully erosion intensified → surface flow erosion → the partial excavation section collapse → slope instability slip → the integral excavation section collapse → the mud water mixture gushes from the tunnel face. Therefore, the slope failure develops gradually from the toe of the slope to the back slope under rainfall condition. The collapse failure of the slope toe and the upper surface of slope first occurs and then develops and gradually aggravates, finally causing the instability and sliding of the whole slope.

(3) The influence of the rainfall infiltration on the tunnel-slope system is characterized by "accumulation." In the early period of the rain, the influence of rainwater infiltration on the stability of the tunnel-slope system is small, but with the continuous rainfall infiltration, the tunnel-slope system will change obviously, and the influence will gradually increase until it is destroyed completely.

(4) By analyzing the change laws of the tunnel-slope system such as displacement, water content, soil pressure, and seepage pressure, it can be concluded that the impact of the rainfall infiltration on the tunnel-slope system presents a certain degree of "hysteresis" characteristic, and the destruction process is gradual. This is one of the important reasons for the instability and destruction of the slope after rain.

Data Availability

The data used to support the findings of this study are available from the corresponding author upon request.

Conflicts of Interest

The authors declare that they have no conflicts of interest.

Acknowledgments

Financial supports from the National Natural Science Foundation of China (42272313), the Key Research and Development Program (Social Development) of Xuzhou City (KC21298), the scientific research project of China Railway Shanghai Group Co., Ltd. (2022178), and the Open Research Fund of State Key Laboratory of Geomechanics and Geotechnical Engineering, Institute of Rock and Soil Mechanics, Chinese Academy of Sciences (Z020014), are sincerely acknowledged.

References

[1] Y. C. Wang, Y. Q. Shang, X. H. Xu, Y. H. Xiao, and X. S. Yan, "Time and space prediction of collapse of loose wall rock at tunnel exit," *Chinese Journal of Geotechnical Engineering*, vol. 32, no. 12, 2010.

[2] M. Zhao, Y. Cheng, Z. Song et al., "Stability analysis of TBM tunnel undercrossing existing high-speed railway tunnel: a case study from Yangtaishan tunnel of Shenzhen metro line 6," *Advances in Civil Engineering*, vol. 2021, Article ID 6674862, 18 pages, 2021.

[3] N. Vlachopoulos, I. Vazaios, and B. M. Madjdabadi, "Investigation into the influence of excavation of twin-bored tunnels within weak rock masses adjacent to slopes," *Canadian Geotechnical Journal*, vol. 55, no. 11, pp. 1533–1551, 2018.

[4] Y. C. Wang, H. W. Jing, H. J. Su, and J. Xie, "Effect of a fault fracture zone on the stability of tunnel-surrounding rock," *International Journal of Geomechanics*, vol. 17, no. 6, 2017.

[5] N. Roy, R. Sarkar, and S. D. Bharti, "Prediction model for performance evaluation of tunnel excavation in blocky rock mass," *International Journal of Geomechanics*, vol. 18, no. 1, p. 04017125, 2018.

[6] F. Huang, H. Zhu, S. Jiang, and B. Liang, "Excavation-damaged zone around tunnel surface under different release ratios of displacement," *International Journal of Geomechanics*, vol. 17, no. 4, p. 04016094, 2017.

[7] P. Gattinoni and L. Scesi, "Lanslide hydrogeological susceptibility of Maierato (Vibo Valentia, Southern Italy)," *Natural Hazards*, vol. 66, no. 2, pp. 629–648, 2013.

[8] S. Miao, X. Hao, X. Guo, Z. Wang, and M. Liang, "Displacement and landslide forecast based on an improved version of Saito's method together with the Verhulst-Grey model," *Arabian Journal of Geosciences*, vol. 10, no. 3, pp. 1–10, 2017.

[9] C. Duenser, K. Thoeni, K. Riederer, B. Lindner, and G. Beer, "New developments of the boundary element method for underground constructions," *International Journal of Geomechanics*, vol. 12, no. 6, pp. 665–675, 2012.

[10] Y. Wang, F. Geng, S. Yang, H. Jing, and B. Meng, "Numerical simulation of particle migration from crushed sandstones during groundwater inrush," *Journal of Hazardous Materials*, vol. 362, pp. 327–335, 2019.

[11] Y. Jing, R. G. Deng, Z. B. Zhong, K. T. Li, and C. P. Sun, "Stress and deformation laws and influence factors analysis of tunnel across the slope deformation zone," *Chinese Journal of Rock Mechanics and Engineering*, vol. 35, no. S2, pp. 3615–3625, 2016.

[12] J. Kumar and P. Bhattacharya, "Reducing the computational effort for performing linear optimization in the lower-bound finite elements limit analysis," *International Journal of Geomechanics*, vol. 11, no. 5, pp. 406–412, 2011.

[13] S. Alemdag, A. Kaya, M. Karadag, Z. Gurocak, and F. Bulut, "Utilization of the limit equilibrium and finite element methods for the stability analysis of the slope debris: an example of the Kalebasi District (NE Turkey)," *Journal of African Earth Sciences*, vol. 106, pp. 134–146, 2015.

[14] S. G. Xiao, C. C. Xia, and D. P. Zhou, "One definition and analysis method of relaxation zone in cutting slope," *Journal of Tongji University*, vol. 33, no. 4, pp. 451–455, 2005.

[15] H. M. Ma, "Discussion on problems of slope disaster and tunnel deformation," *Chinese Journal of Rock Mechanics and Engineering*, vol. 22, no. S2, pp. 2719–2724, 2003.

[16] Z. P. Tao, *Study on Tunnel Deformation on Mechanism at Landslide Site and Disaster Predicting and Controlling*, Southwest Jiaotong University, 2003.

[17] H. Wu, *Research on Deformation Mechanism and Control Technology of Tunnel-Landslide System*, China Academy of Railway Sciences, 2012.

[18] A. Kaya, A. Akgün, K. Karaman, and F. Bulut, "Understanding the mechanism of slope failure on a nearby highway tunnel route by different slope stability analysis methods: a case from NE Turkey," *Bulletin of Engineering Geology and the Environment*, vol. 75, no. 3, pp. 945–958, 2016.

[19] R. L. Baum, J. W. Godt, and W. Z. Savage, "Estimating the timing and location of shallow rainfall-induced landslides using a model for transient, unsaturated infiltration," *Journal of Geophysical Research: Earth Surface*, vol. 115, no. F3, 2010.

[20] L. Henry and I. Hoe, "Centrifuge model simulations of rainfall-induced slope instability," *Journal of Geotechnical and Geoenvironmental Engineering*, vol. 138, no. 9, pp. 1151–1157, 2012.

[21] S. Ganger, *Duzhengliang and Xiaoqiaochengzhi (Japanese). "Landslide and Slope Failure and Its Prevention and Control."*, Science Press, Beijing, 1980.

[22] Z. P. Tao and D. P. Zhou, "Model test on deformation mechanism of tunnel at land-slide site," *Journal of Engineering Geology*, vol. 2003, no. 3, pp. 323–327, 2003.

[23] H. G. Wu, X. Y. Chen, and H. Ai, "Research on the deformation mechanism model test of tunnel-landslide parallel system," *Journal of Railway Engineering Society*, vol. 33, no. 11, 2016.

[24] H. G. Wu, X. Y. Chen, and H. Ai, "Research on the deformation mechanism model test of tunnel-landslide skew system," *Journal of Railway Engineering Society*, vol. 33, no. 9, 2016.

[25] H. G. Wu, X. Y. Chen, and H. Ai, "Research on the force exerting mode model test of tunnel-landslide orthogonal system," *Journal of Railway Engineering Society*, vol. 3, 2016.

[26] Z. H. G. Zhang, C. P. Zhang, B. B. Ma, J. F. Gong, and T. Ye, "Physical model test and numerical simulation for anchor cable reinforcements of existing tunnel under action of landslide," *Rock and Soil Mechanics*, vol. 39, no. S1, pp. 51–60, 2018.

[27] J. Yin, R. G. Deng, K. T. Li, B. J. Chen, and C. H. P. Sun, "Stress and deformation of self-anchored reinforcement structures for landslide tunnels," *Chinese Journal of Rock Mechanics and Engineering*, vol. 35, no. 10, pp. 2062–2079, 2016.

[28] J. B. Chen, "Experimental study on the influence of engineering disturbance on the tunnel-landslide orthogonal system," *Value Engineering*, vol. 36, no. 24, pp. 133–136, 2017.

[29] H. Ai, H. G. Wu, and X. Y. Chen, "Research on the influence mechanism of rainfall for the tunnel-landslide orthogonal system without the supporting structure," *China Earthquake Engineering Journal*, vol. 39, no. 2, pp. 0213–0220, 2017.

[30] Y. Gao, H. Wei, and B. Li, "Disaster evolution mechanism of rainfall-landslide-tunnel system: a case study of Yangjiawan tunnel of Fengxi highway in Chongqing," *Tunnel Construction*, vol. 42, no. 4, 2022.

[31] L. Li, C. H. He, P. Geng, and D. J. Cao, "Study of shaking table model test for seismic response of portal section of shallow unsymmetrical loading tunnel," *Chinese Journal of Rock Mechanics and Engineering*, vol. 30, no. 12, pp. 2540–2548, 2011.

[32] E. Yalcin, Z. Gurocak, R. Ghabchi, and M. Zaman, "Numerical analysis for a realistic support design: case study of the Komurhan tunnel in eastern Turkey," *International Journal of Geomechanics*, vol. 16, no. 3, 2016.

[33] J. X. Wang, H. H. Zhu, Y. Q. Tang, L. S. Hu, P. Yang, and D. Wu, "Interaction between twin-arc tunnel and slope: twin-arc tunnel landslide," *China Civil Engineering Journal*, vol. 43, no. 1, pp. 103–107, 2010.

[34] Y. Xing, P. H. S. W. Kulatilake, and L. A. Sandbak, "Stability assessment and support design for underground tunnels located in complex geologies and subjected to engineering activities: case study," *International Journal of Geomechanics*, vol. 19, no. 5, p. 05019004, 2019.

[35] Q. Zhang, J. Wang, W. Wang, S. Bai, and P. Lin, "Study on slope stability due to the influence of excavation of the high-speed rail tunnel," *Geomatics, Natural Hazards and Risk*, vol. 10, no. 1, pp. 1193–1208, 2019.

[36] P. Gattinoni, M. Consonni, V. Francani, G. Leonelli, and C. Lorenzo, "Tunnelling in landslide areas connected to deep seated gravitational deformations: an example in Central Alps (northern Italy)," *Tunnelling and Underground Space Technology*, vol. 93, article 103100, 2019.

[37] L. Qin, *Analysis of Slope Stability Influenced by Tunnel Excavation: A Study of Reinforcement Measures*, Central South University, 2012.

[38] H. Moriwaki, T. Inokuchi, T. Hattanji, K. Sassa, H. Ochiai, and G. Wang, "Failure processes in a full-scale landslide experiment using a rainfall simulator," *Landslides*, vol. 1, no. 4, pp. 277–288, 2004.

[39] J. W. Hu, *The Stability Evaluation and Treatment Measures for the Daping No. III Landslide*, Chang'an University, 2013.

[40] S. F. Wang, *Fengjie Daping Landslide in Chongqing City Stability Analyses and Government Plan Discussion*, Xi'an University of Science and Technology, 2008.

[41] S. Sun and Y. Zhang, "Similarity criterion in physical simulation of rainfall and sheet flow," *Transactions of the Chinese Society of Agricultural Engineering*, vol. 28, no. 11, pp. 93–98, 2012.

[42] Y. Wang, F. Chen, W. Sui, F. Meng, and F. Geng, "Large-scale model test for studying the water inrush during tunnel excavation in fault," *Bulletin of Engineering Geology and the Environment*, vol. 81, no. 6, 2022.

[43] Y. C. Wang, Y. Liu, N. Zhao, and W. Jiang, "Investigation on the evolution mechanism of water and mud inrush disaster in fractured rock mass of mountain tunnel," *Geomatics, Natural Hazards and Risk*, vol. 13, no. 1, pp. 1780–1804, 2022.